On the optical, structural, and morphological properties of ZrO$_2$ and TiO$_2$ dip-coated thin films supported on glass substrates

Luisa F. Cueto [a], Enrique Sánchez [a], Leticia M. Torres-Martínez [a,*], Gustavo A. Hirata [b]

[a]*Facultad de Ciencias Químicas, División de Estudios Superiores, Universidad Autónoma de Nuevo León, A.P. 1864, Monterrey, N.L., México*
[b]*Centro de Ciencias de la Materia Condensada, UNAM, Km. 107 Carr. Tij.-Ens., Ensenada, B.C., 22860, México*

Abstract

This article reports the optical and morphological properties of dip-coated TiO$_2$ and ZrO$_2$ thin films on soda-lime glass substrates by metal-organic decomposition (MOD) of titanium[IV] and zirconium[IV] acetylacetonates respectively. Thermogravimetric and differential thermal analysis (DTA–TG) were performed on the precursor powders, indicating pure TiO$_2$ anatase and tetragonal ZrO$_2$ phase formation. Phase crystallization processes took place in the range of 300–500 °C for anatase and of 410–500 °C for ZrO$_2$. Fourier Transform Infrared Spectroscopy (FT-IR) was used to confirm precursor bidentate ligand formation with keno-enolic equilibrium character. Deposited films were heated at different temperatures, and their structural, optical and morphological properties were studied by grazing-incidence X-ray Diffraction (GIXRD) and X-Ray Photoelectron Spectroscopy (XPS), Ultraviolet Visible Spectroscopy (UV-Vis), and Atomic Force Microscopy (AFM) respectively. Film thinning and crystalline phase formation were enhanced with increasing temperature upon chelate decomposition. The optimum annealing temperature for both pure anatase TiO$_2$ and tetragonal ZrO$_2$ thin films was found to be 500 °C since solid volume fraction increased with temperature and film refractive index values approached those of pure anatase and tetragonal zirconia. Conditions for clean stoichiometric film formation with an average roughness value of 2 nm are discussed in terms of material binding energies indicated by XPS analyses, refractive index and solid volume fraction obtained indirectly by UV-Vis spectra, and crystalline peak identification provided by GIXRD.
© 2005 Elsevier Inc. All rights reserved.

Keywords: Dip-coated thin films; Metal-organic decomposition (MOD); Titanium oxide (TiO$_2$); Zirconium oxide (ZrO$_2$)

1. Introduction

Ceramic and metallic thin-film coatings on inert substrates have been of recent interest due to their novel and unique properties, proving to be better than those of the substrate and the ceramic coating material by themselves, such as of powders obtained by tradi-

* Corresponding author. Tel.: +52 81 83321902x112; mobile: +52 81 83665054; fax: +52 81 83760477.
E-mail addresses: lettorresg@yahoo.com, ltorres@ccr.dsi.uanl.mx (L.M. Torres-Martínez).

tional high-temperature methods [1–6]. Some of these properties, such as film transparency and homogeneity are important for optical applications and have been successfully obtained by the dip and spin coating method [4,6,7]. More sophisticated physical deposition methods, such as laser ablation and combustion, have been used to grow luminescent films [8], achieving epitaxial growth with the additional good control of desired material properties. On the other hand, dip and spin coating are simpler and more convenient film-growing methods that produce materials with desirable properties for some applications, such as the photocatalytic degradation of pollutants [4,5].

Among ceramic materials that have been widely studied, titanium[IV] oxide (TiO_2, titania) thin film coatings is one of the main representatives. It has been successfully applied to heterogeneous photocatalysis for the oxidation of volatile organic contaminants from effluents into environmentally safe products [4]. Recently, it has been applied as a material exhibiting self-cleaning, anti-fogging and anti-bacterial properties [5,6]. Zirconium[IV] oxide (ZrO_2, zirconia) is well known for its good mechanical properties [9]. When it is part of the film, it enhances film endurance in applications where the material must undergo extreme conditions [10]. As a bifunctional catalyst, it is useful in the selective synthesis of α-olefins from alcohols, the synthesis of 1-butene from 2-butanamine, as well as in the reduction reactions of aldehydes, ketones, carboxylic acids, and esters with alcohols; and also in the isosynthesis process [10]. Moreover, some research groups have studied zirconium dioxide catalytic properties, promoting its super acid behavior by sulfatation [11].

In this work, the growth of titanium[IV] and zirconium[IV] oxide thin films deposited on both sides of glass substrates by the dip-coating method is reported [12]. Their optical properties, calculated from Ultraviolet-Visible Spectroscopy (UV-Vis) transmittance spectra [1,13], revealed that film thickness decreases with heating temperature. Grazing-incidence X-Ray Diffraction (GIXRD) studies showed that TiO_2 (anatase) and tetragonal ZrO_2 were successfully coated on the substrate. X-Ray Photoelectron Spectroscopy (XPS) measurements showed good film stoichiometry and Atomic Force Microscopy (AFM), revealed a smooth surface with roughness value of 2 nm for both materials.

2. Experimental section

2.1. Chemical reagents and substrates

All commercial, extra pure reagents were used as received. Titanium n-butoxide ($Ti(OBu^n)_4$), TNB (97 wt.% in butyl alcohol), and 2,4-pentenedione (acetylacetone, acacH) were used from Sigma-Aldrich Chemical Company, Inc. Zirconium n-butoxide ($Zr(OBu^n)_4$), ZNB, (80 wt.% in *tert*-butanol) was used from Fluka Chemie AG, and absolute ethyl alcohol from CTR Scientific. Soda lime glass microscope slides, Corning No. 2947, were used as substrates.

2.2. Precursor characterization

Titanium and zirconium acetylacetonates were characterized by Fourier Transform Infrared Spectroscopy (FT-IR) using a Perkin Elmer Paragon 1000 PC FT-IR Spectrometer. Their isolated powders were analyzed by Differential Thermal Analysis–Thermogravimetric (DTA–TG) studies, using a TA Instrument Simultaneous Thermal Analyzer SDT-2960.

2.3. Film characterization

Oxide films refractive index and thickness were examined by UV-Vis Spectroscopy using a Perkin Elmer Lambda 12 conventional UV Vis Spectrometer. GIXRD patterns were obtained with a Siemens D-5000 Diffractometer using LiF monochromated CuKα radiation using a step time of 3 s and a stepsize of $0.02°$ at an accelerating voltage 40 kV and applied current of 30 mA were taken over the 2θ range of 5–90°. Optical quality of the films was examined using an Olympus BX60F5 Optical Microscope with polarized light accessory and HITACHI KP-050 Digital Camera. Film topography was observed using an Atomic Force Microscope (AFM) from Digital Instruments. A Multimode Scanning Probe QUESANT Qscope-250 was used operated in air at room temperature. X-ray Photoelectron Spectroscopy (XPS) analyses were performed on film surface in order to determine the chemical states of zirconium and titanium oxides. The XPS analysis was carried out on a spectrometer (Riber II) using AlKα as the excitation source. The electron analyzer was operated at a constant energy

pass of 50 eV. Calibration of the binding energy scale as well as correction of the energy shift as a result of the steady-state charging effect of the C1s line lying at 284.6 eV was performed.

2.4. Reaction of metal alkoxides with acetylacetone

The reaction of each metal alkoxide with acacH was carried out at room temperature in air. A molar relationship 2:1 of acacH:alkoxide were dissolved in ethyl alcohol to obtain approximate metal molar concentrations of 0.5–0.6 M. The solutions were stored at room temperature, closely capped to prevent their contact with air and humidity [7].

2.5. Thin film formation

The dipping process was carried out at room temperature under an air atmosphere. The substrates were put in a vertical position, tightly held by a dipping holder. Both sides of substrates were immersed for a 30-min period, and pulled up at a rate of 3 to 5 cm/min. The solvent was allowed to evaporate for 30 min and then the samples were fired using two different heating methods. In the first method, samples were heated at a rate of 1 °C/min from room temperature to 150, 300 and 500 °C [7]. In each case, temperature was held for 10 min, and finally cooled down to room temperature at the same temperature rate. In the second method, the samples were directly introduced inside the furnace, heated for 30 min, removed from the furnace, and put into a dessicator for cooling them down to room temperature [7].

3. Results and discussion

3.1. Reaction of metallic alkoxides with acetylacetone

The general form of the chemical reaction that took place between metal alkoxides and acetylacetone is represented by the equation

$$M(OR)_4 + 2acacH \rightarrow M(OR)_{4-x}(acac)_x + xROH. \qquad (1)$$
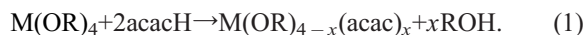
The alkoxy groups R are displaced by the acetylacetone molecule forming a stabilized chelate coordination compound [12,13]. In the present investigation,

M = Ti or Zr, and R = CH_3–CH_2– or CH_3–$(CH_2)_3$– since some substitution of butoxide (–OBu) groups by ethoxy (–OEt) groups may occur as the alkoxide is dissolved in ethanol without affecting the condensation reaction of the process.

3.2. Metal complex formation

The obtained FT-IR spectra of the titanium and zirconium complexes are shown in Fig. 1(a) and (b) respectively.

The peaks at 3300–3400 cm^{-1} correspond to solvent hydroxyl group vibration [14]. Signals ranging
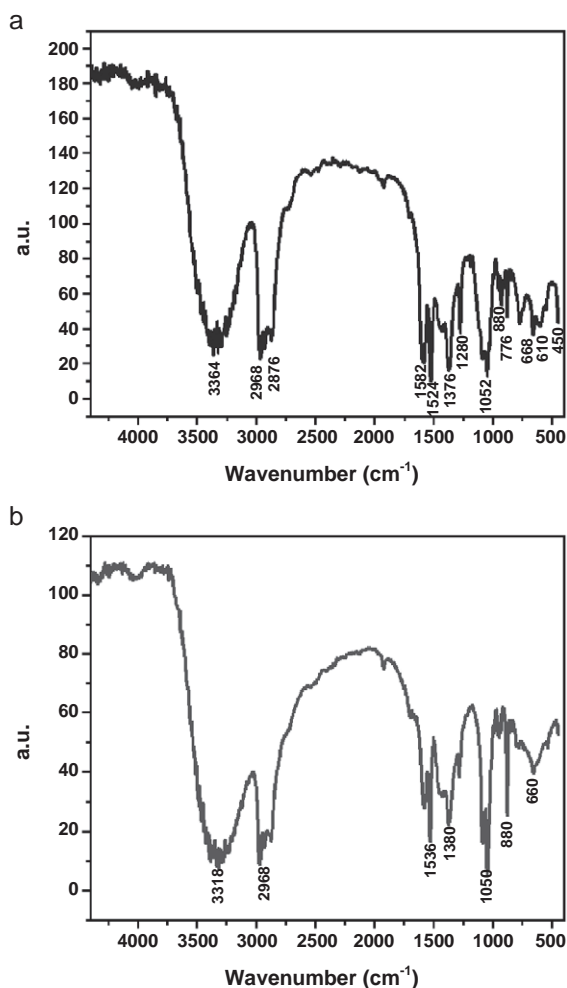
Fig. 1. (a) FT-IR spectrum of Ti(OBu)$_{4-x}$(acac)$_x$, [Ti] ≈ 0.6M, (b) FT-IR spectrum of Zr(OBu)$_{4-x}$(acac)$_x$, [Zr] ≈ 0.5M.

from approximately 2970 and 2880 cm^{-1} belong to alkane groups present in the complex. The most relevant peak in all spectra, ranging from 1650–1530 cm^{-1} indicated the formation of a bidentante complex with keto-enolic equilibrium behavior. This denotes evident ring formation and coordination of the metal with acetylacetone carbonyl groups with resonant character. This behavior was confirmed by peaks near to 1000 cm^{-1} corresponding to M=O and C=C–C vibrations, which gave important information about the formation of a bidentate species, a cycle with acetylacetone framework in coordination with the metal. Peaks below 610 cm^{-1} indicated M–O bond vibrations, which confirmed the proposed acetylacetonate structures. The differences in wave number associated to functional groups in each case were displacements mainly due to each alkoxide chemical nature, such as their reactivity with acetylacetone as a function of their ionic radius. This is closely associated with the coordination number of the metal and its capability to coordinate a specific number of aceylacetone molecules. In the case of titanium and zirconium complexes, zirconium can coordinate more acacH molecules than titanium, due to atomic size difference. Based on previous information on alkoxide-stabilizing complex formation, these compounds are regarded as metal acetylacetonates with the formula $(C_5H_7O_2)_2OTi$ for the titanium complex and $(C_5H_7O_2)_4Zr$ for the zirconium complex [13].

3.3. Estimation of thin films optical properties

At a wavelength range of 1100 to 280 nm (in which transmittance for glass is zero) optical properties measures can be performed since on evaluating film thickness and refractive index values from optical data, the most important fact to consider is that both film and substrate have no light absorption in the wavelength region of performed measurements [1,13,15,16].

Light, which passes a both-side film experiences infinite reflection at those interfaces, each interface having reflection R. Illuminated light is reflected at the first interface, thus transmitting $1 - R$. This is reflected at the second interface by R, lowering the transmittance by $R(1 - R)$. But this reflected light is again reflected at the first interface, intensifying the transmittance [15,16]. Then, transmittance T can be

written as $T = (1-R)-R(1-R)+R^2(1-R)-R^3(1-R)+ \ldots + R^{n-1}(1-R)-R^n(1-R)$. $R^2(1-R)$ may be again reflected at the second interface, reducing the transmittance by $R^3(1-R)$ and then at the first interface transmittance will be increased by $R^4(1-R)$, and so on. Transmittance $T = (1-R)[1-R+R^2-R^3+\ldots+R^{n-1}-R^n]$. Here, $R < 1$, then $T(1-R)/(1+R)$, and $R = (1-T)/(1+T)$, applicable to a both-side coated substrate (only for dip-coated substrates).

By analyzing resulting minima and maxima signals of a UV-Vis transmittance (%T) vs. wavelength (λ) spectra caused by interference phenomena of incident light with the film, Eq. (2) may be used to estimate optical parameters [15,16]

$$R = \frac{(n_0 - n_s)^2\cos^2\pi\delta + [(n_0 n_s/n_f) - n_f]^2\sin^2\pi\delta}{(n_0 + n_s)^2\cos^2\pi\delta + [(n_0 n_s/n_f) + n_f]^2\sin^2\pi\delta} \qquad (2)$$

where n_0 is the refractive index of air, n_s is the refractive index of the substrate (1.52 for soda-lime glass), n_f is the refractive index of the film, and $\delta = 2n_f d\cos\theta/\lambda$ (where d is film thickness, θ is the angle of incidence, and λ is the wavelength corresponding to the maximum or minimum signals in the spectrum).

For film volume fraction estimation (V_f) – the ratio of the volume in which the solid substance constitutes the films – may be done with the Lorentz–Lorentz relationship. It relates obtained film and pure substance refractive indexes – indicated by MO_2 in Eq. (3) – (e.g. anatase or tetragonal ZrO_2) in the following way [15]:

$$V_f = \frac{(n_f^2 - 1)(n_{MO_2}^2 + 2)}{(n_{MO_2}^2 - 1)(n_f^2 + 2)}. \qquad (3)$$

The obtained UV-Vis spectra for TiO_2 and ZrO_2 films are shown in Fig. 2(a) and (b) respectively. As a result of a single coating application, very broad valleys were found in both graphs and a low number of maxima and minima could be identified. Table 1 compares refractive index, thickness and volume fraction of the studied materials at different temperatures [15]. Unheated samples were four to five times thicker than heated ones. Unheated ZrO_2 films appeared thicker than unheated TiO_2 films, suggesting precursor higher reactivity and viscosity as a result of larger
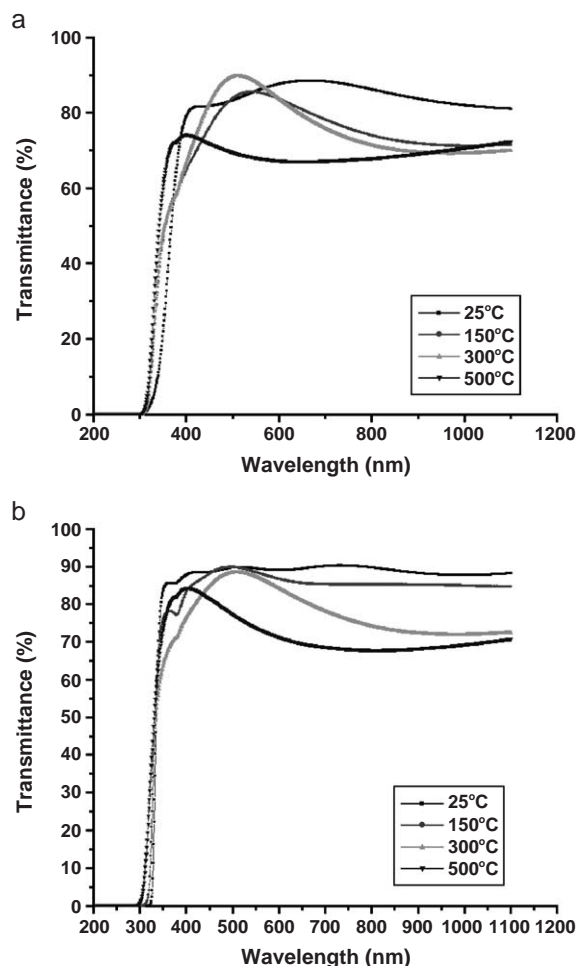
Fig. 2. (a) UV-Vis spectra of TiO_2 supported on soda lime glass substrates. (b) UV-Vis spectra of ZrO_2 supported on soda lime glass substrates.

Table 1
Refractive index (η_f), solid volume fraction (V_f) and thickness (d) of TiO_2 and ZrO_2 thin films as a function of temperature

	TiO_2			ZrO_2		
	η_f	V_f	d(nm)	η_f	V_f	d(nm)
25 °C	1.58 ($\lambda=673$ nm)	0.519	425	1.57 ($\lambda=607$ nm)	0.618	480
150 °C	1.63 ($\lambda=545$ nm)	0.556	166	1.64 ($\lambda=718$ nm)	0.678	327
300 °C	1.56 ($\lambda=511$ nm)	0.500	124	1.58 ($\lambda=507$ nm)	0.625	130
500 °C	1.98 ($\lambda=653$ nm)	0.767	82	1.66 ($\lambda=403$ nm)	0.691	121

heat treatment was applied, indicating a low volume fraction and a vast porous region. This low volume fraction, around 48% for titania and 38% for zirconia, can be explained in terms of precursor initial concen-
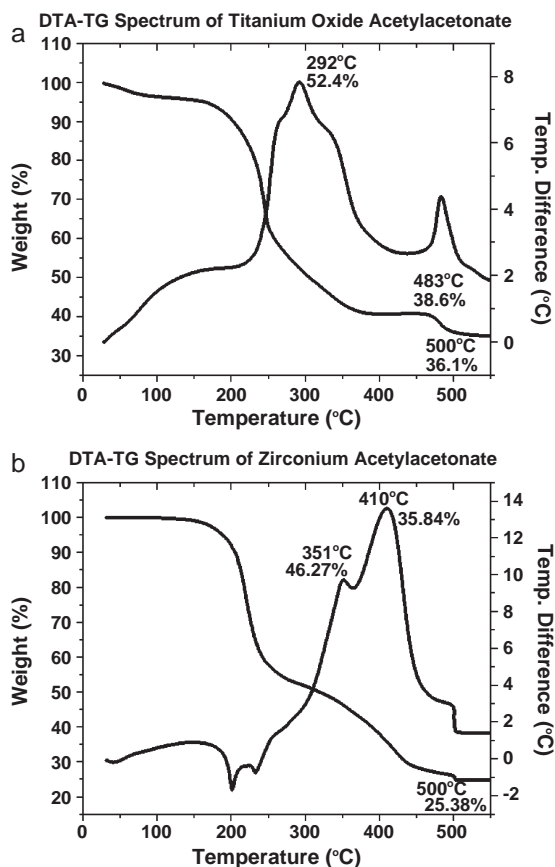
Fig. 3. (a) DTA–TG behavior curves of titanium[IV] and acetylacetonate. (b) DTA–TG behavior curves of zirconium[IV] acetylacetonate.

amounts of acetylacetone required to stabilize the zirconium alkoxide [13]. The DTA–TG curves for the combustion process of dried powders of titanium and zirconium acetylacetonates are shown in Fig. 3(a) and (b) respectively. Crystallization of zirconium[IV] acetylacetonate began at 410 °C and completed at 500 °C, indicated by the exothermic peak. Crystallization temperature of titanium[IV] oxide began at approximately 300 °C, and anatase phase formation of TiO_2 took place at 500 °C. In the two cases, weight difference acquainted for TiO_2 and ZrO_2 formation and no further weight changes were registered at higher temperatures. In both titania and zirconia films, the greatest transparency was found before

a

b

Fig. 4. (a) Grazing-angle X-Ray Diffraction patterns of TiO_2 (anatase) thin films formed at 500 °C on soda lime glass substrates. (b) Grazing-angle X-Ray Diffraction patterns of tetragonal ZrO_2 thin films formed at 500 °C on soda lime glass substrates.

tration, 0.5 M for titanium and 0.6 M for zirconium acetylacetonates. As temperature was applied, the refractive index of the films increased, getting closer to the values reported for pure anatase (2.54) and zirconia (~2.11) [16]. This behavior indicates phase formation that accounts for the decrease in transparency due to the material presence in the substrate. Film thickness decreased proportionally with temperature upon decomposition of the chelate, yielding the desired oxide deposited on the substrate. Optimum temperature resulted to be 500 °C in terms of film thickness, trans-

parency, volume fraction, desired phase formation (exclusively anatase TiO_2 and tetragonal ZrO_2) [18] and the prevention of substrate softening [17].

3.4. Thin film structure and morphology

The structural and morphological features of these films were studied as a function of the growth and heating conditions by Optical and Atomic Force Microscopy and X-Ray Diffraction. Fig. 4 shows XRD patterns measured at low angles for (a) TiO_2 (anatase) and (b) ZrO_2 (tetragonal) films supported on glass substrates and heat-treated at 500 °C. Phase formation was expected for metal acetylacetonates

a

b
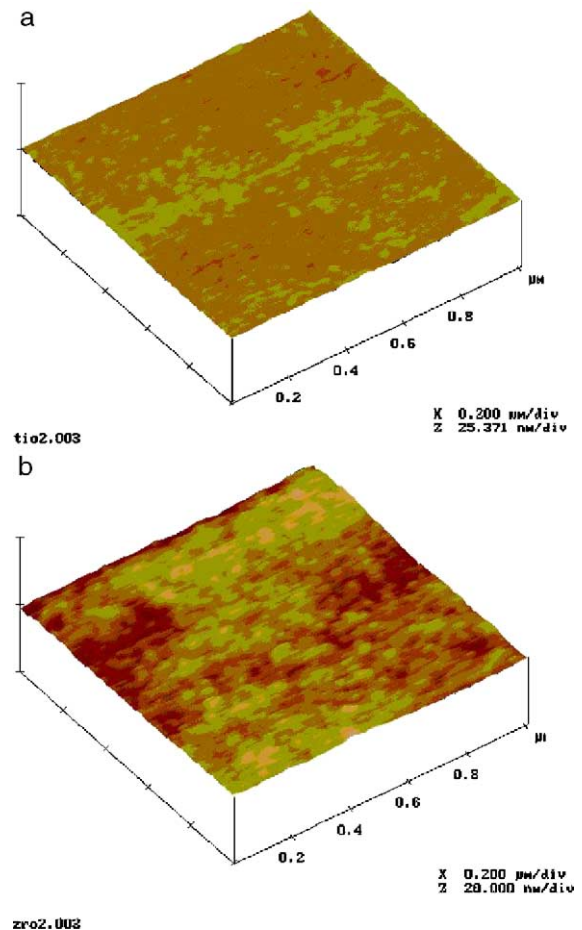
Fig. 5. (a) Surface topography of titanium oxide film formed at 500 °C with a roughness value around 2 nm. (b) Surface topography of zirconium oxide film formed at 500 °C with a roughness value around 2 nm.

combustion at low temperatures. However, peaks corresponding to sodium chloride appeared in both cases, indicating Na^+ ion diffusion into the film as reported by others [3]. This might be due to sodium ion small size along with the slow-heating process that was applied, enabling its movement from the substrate into the film.

XPS of TiO$_2$ prepared at 500°C

XPS of ZrO$_2$ film prepared at 500°C
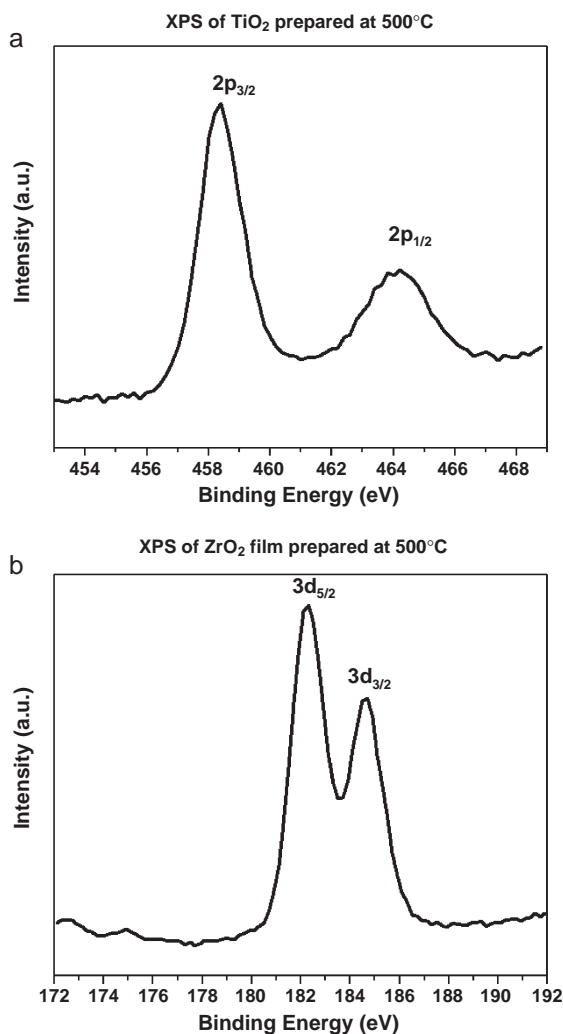
Fig. 6. (a) XPS analysis on TiO$_2$ thin film surface, showing the typical Ti2p$_{3/2}$ – Ti2p$_{1/2}$ doublet and a binding energy around 458 eV, corresponding to the reported value for Ti–O bonding. This film was formed at 500 °C, (b) XPS analysis on ZrO$_2$ thin film surface, showing the typical Zr3d$_{5/2}$ – Zr3d$_{3/2}$ doublet and a binding energy around 182 eV, corresponding to the reported value for Zr–O bonding. This film was formed at 500 °C.

In addition, very different optical quality of the films was observed with different heating rates. Films fired at slow heating rates showed fractures and a few nuclei, while samples heated directly at 500 °C did not show either fractures or nuclei. Their morphology was different, allowing the formation of more homogeneous films at greater heating rates.

The topographies of the titanium oxide and zirconium oxide films studied by AFM are depicted in Fig. 5(a) and (b). It can be seen from topographic measurements that relatively small and regular grains were obtained in both cases for the optimum formation temperature at 500 °C. An average roughness value of around 2 nm was measured for 500 °C heated films.

X-Ray Photoelectron Spectroscopy (XPS) analyses performed on the surfaces of the TiO$_2$ and ZrO$_2$ thin films formed at 500 °C and the results are given in Fig. 6(a) and (b), respectively. Fig. 6(a) shows the XPS data of Ti2p spectrum with the Ti2p$_{3/2}$ – Ti2p$_{1/2}$ typical doublet. It can be observed that the peak at ~458 eV corresponds to the reported value for Ti–O bonding, while Fig. 6(b) gives the Zr3d$_{5/2}$ – Zr3d$_{3/2}$ doublet showing the Zr–O bonding around 182 eV [19]. In both cases, the shape of the spectra and the position of the peaks (binding energies) clearly indicated the formation of stoichiometric titanium[IV] and zirconium[IV] oxides by the dip-coating method used in the present investigation.

4. Conclusions

Titanium[IV] and zirconium[IV] oxide thin films supported on both sides of soda lime glass substrates were prepared by metal-organic decomposition of bidentate ligand keto-enolic titanium[IV] and zirconium[IV] acetylacetonate precursors. Both TiO$_2$ and ZrO$_2$ films showed similar thermal behavior as indicated by DTA–TG analyses. Despite the low firing temperatures of the samples, anatase TiO$_2$ and tetragonal ZrO$_2$ were identified from GIXRD. Film thickness and refractive index, indirectly calculated using UV-Vis transmittance spectra, decreased with firing temperature, and solid volume fraction estimated by the Lorentz–Lorentz relationship increased with temperature, indicating film thinning and expected phase formation, leaving homogeneous, transparent films. Smooth

films with a roughness value of around 2 nm were obtained for titania and zirconia as shown by Atomic Force Microscopy. Heating conditions considerably affected film optical appearance and morphology, for which samples directly heated at 500 °C showed the best film homogeneity and crack-free appearance, while multiple cracks and nuclei were shown when samples were heated at slow rates. Formation temperature at 500 °C resulted in the optimum condition to obtain clean stoichiometric TiO_2 and ZrO_2 thin films on glass substrates as confirmed by X-Ray Photoelectron Spectroscopy measurements.

Acknowledgements

References

[1] Takahashi Y, Ohsugi A, Arafuka T, Ohya T, Ban T, Ohya Y. Development of new modifiers for titanium alkoxide-base sol–gel process. J Sol-Gel Sci Technol 2000;17:227–38.

[2] Smith DL. Thin-film deposition. Principles and practice. New York, NY: McGraw-Hill, Inc.; 1995. p. 1.

[3] Watanabe T, Fukayama S, Miyauchi M, Fujishima A, Hashimoto K. J Sol-Gel Sci Technol 2000;19:71.

[4] Blount MC, Kim DH, Falconer JL. Transparent thin-film TiO_2 photocatalysts with activity. Environ Sci Technol 2001;35:2988–94.

[5] Zorn ME, Tompkins DT, Zeltner WA, Anderson MA. Catalytic and photocatalytic oxidation of ethylene on titania-based thin-films. Environ Sci Tech 2000;34:5206–10.

[6] Ohya T, Nakayama A, Ban T, Ohya Y, Takahashi Y. J Sol-Gel Sci Technol 2002;14:3082.

[7] Tada H, Tanaka M. Dependence of TiO_2 photocatalytic activity upon its film thickness. Langmuir 1997;13:360–4.

[8] Hirata GA, McKittrick J, Avalos-Borja M, Siqueiros JM, Devlin D. Appl Surf Sci 1997;113/114:509.

[9] Marshall D, Shaw M, Dauskardt R, Ritchie R, Ready M, Heuer A. J Am Ceram Soc 1990;73:2659.

[10] Tanabe K, Yamaguchi T. Catal Today 1994;20:185.

[11] Lopez T, Tzompantzi F, Hernandez-Ventura J, Gomez R. Effect of zirconia precursor on the properties of ZrO_2–SiO_2 sol–gel oxides. J Sol-Gel Science Technol 2002;24:207–19.

[12] Brinker CJ, Scherer GW. Sol–gel science: the physics and chemistry of sol–gel processing. London, UK: Academic Press, Inc; 1990. p. 43.

[13] Ohya T, Kabata M, Ban T, Ohya Y, Takahashi Y. J Sol-Gel Science Technol 2002;25:43.

[14] Nakamoto K. Infrared and raman spectra of inorganic and coordination compounds. New York, NY: John Wiley and Sons, Inc.; 1978. p. 249.

[15] Yoshida S, Yajima G. Optical thin films and devices. Tokyo: University of Tokyo Press; 1994.

[16] Macleod HA. Thin film optical filters. Third Edition. London, UK: Institute of Physics Publishing; 2001. p. 12–85.

[17] Barsoum MW. Fundamentals of ceramics. Cornwall: Institute of Physics Publishing Ltd; 2003. p. 558.

[18] Levin EM, McMurdie HF. Phase diagrams for ceramists. The American Ceramic Society; 1975.

[19] Moulder JF, Stickle WF, Sobol PE, Bomben KD. Handbook of X-Ray photoelectron spectroscopy: a reference book of standard spectra for identification and interpretation of XPS data. Eden Prairie: Perkin-Elmer Corporation - Physical Electronics Division; 1993, p. 38–46, 48, 50, 51, 63, 72, 73, 124–127.

Professor Dr. Leticia M. Torres-Martínez PROFESSIONAL EXPERIENCE—She leads and founded the Center of Research and Development of Ceramic Materials (CIDEMAC), which is located in the Faculty of Chemistry, at Universidad Autónoma de Nuevo León, México. CIDEMAC was nominated as a finalist at the 2000 National Technology Awards convened by the Ministry of the Trade and Industrial Development and the Mexican Republican Presidence.

She has been leader in different or several technological projects of National Ceramic Industry.

She designed, structured and implemented two graduate programs (MSc and PhD) in ceramic engineering, which has the recognition of the federal government as an excellent or high level graduate program. She has directed 42 graduate students and currently directs 12 theses. She has designed a similar graduate programs offered to two big industries of cement (CEMEX, S.A. de C.V.) and glass (VITRO S.A. de C.V.).

She has been coordinator in the last four years of homologous research groups (ceramic materials) in order to carry out different technological projects of the national ceramic industry.

She has got more than 40 awards from national and international organizations, including 12 awards for best research work of the University of Nuevo Leon (Science and Technology) in the last 10 years.

She has been leader in several technological projects of National Ceramic Industry.

She was Invited Editor for the Special Issue: Inorganic Chemistry in Latin America edited by Polyhedron. In addition, she has contributed with the Journal of Solid State Chemistry as Coordinator in Latin America for the Special Issue on Solid State Science.

RESEARCH INTERESTS—

- Synthesis and Characterization of Novel Functional Materials (Phase Equilibrium Diagrams).
- Electrical, Electrochemical, Catalytic and Photocatalytic Properties.
- Ceramics Materials Development for Environmental Photocatalysis (Water and Soil Remediation, water splitting hydrogen generation).

PUBLICATIONS—
Professor Torres-Martínez has around 100 scientific papers and 35 extended abstract (indexed).
Some selected research publications:

1. Sol–Gel Titania Modified with Ba and Li Atoms for Catalytic Combustion. T. Lopez, A. Hernández, X. Bokhimi, L. Torres, A. García, G. Pecchi. Journal of Materials Sciences, Vol. 39 (2004), 565–570.
2. Photocatalytic Behavior of the Ceramics Compounds with Similar Structures: $Ba_3Li_2Ti_8O_{20}$, $A_mM_{2n}O_{4n+1}$ (A=Li, Na, K; m=2, n=3). Adv. In Tech, of Mat. And Mat Proc. J. (ATM). Vol.6 [2] 184–191 (2004).
3. Alternative Batch Compositions in the Glass Forming Region of the Na_2O–CaO–SiO_2 System. B. Garza Montoya, L.M. Torres-Martínez, P. Quintana, J. Ibarra. Journal of Non-Crystalline Solids, Vol. 329, No. 1–3, pp 22–26 (2003).

4. Crystallization Kinetics and Phase Transformation of xLi_2S–$(1-x)Sb_2S_3$, x=0–0.17 Glass. S. de la Parra, L.C. Torres-Gonzalez, L.M. Torres-Martínez and E. Sánchez. Journal of Non-Crystalline Solids, Vol. 329, No.1–3, pp 105–108 (2003).
5. Kinetic Thermal Analysis of Glass Ceramics from Industrial Wastes. A. Alvarez-Mendez, L.C. Torres-Gonzalez, N. Alvarez, L.M. Torres-Martinez. Journal of Non-Crystalline Solids, Vol. 329, No. 1–3, pp 74–77 (2003).
6. Ceramic Compounds $M_2Ti_nO_{2n+1}$ (M=Li, Na, K y n=2), Synthesis and Photocatalytic Properties. Aracely Hernández, Leticia M. Torres Martínez, Wendy Ortega, Tessy López. Emerging Fields in Sol–gel Science and Technolgy. Kluwer Academy Publishers 2003, pp. 84–91, Boston. Hardbound ISBN-1-4020-7458-1.
7. Synthesis of $Ba_3Li_2Ti_8O_{20}$ Sol–Gel at Basic Conditions. Aracely Hernandez, Leticia M. Torres-Martinez, Tessy Lopez. Materials Letters, 54 (2002) 62–69.
8. Subsolidus Phase Equilibria in the System CaO–Al_2O_3–CoO and the Crystal Structure of Novel $Ca_3CoAl_4O_{10}$. B. Vazquez, L. Torres-Martínez, N. Alvarez, J.F. Vente and P. Quintana. Journal of Solid State Chemistry, 166, 191–196 (2002).
9. Photocatalytic properties of $Ba_3Li_2Ti_8O_{20}$ sol–gel. A. Hernandez, L.M. Torres-Martinez, E. Sánchez-Mora, T. Lopez and F. Tzompantzi. Journal of Materials Chemistry 2002, 12, 1–6.
10. A Study of the Crystallization of ZrO_2 in the Sol–Gel System: ZrO_2–SiO_2. D.H. Aguilar, L.C. Torres-González, L.M. Torres-Martínez, T. López and P. Quintana. Journal of Solid State Chemistry, Vol. 158, 349–357 (2001).
11. Phase Formation and Electrical Properties in the System BaO–Li_2O–TiO_2. Journal of Materials Chemistry, (1994) 4 (1), 5–8.